

# Effect of Nano-Sized Oxides on Annealing Behaviour of Ultrafine Grained Steels

Andrey Belyakov, Yoshikazu Sakai, Toru Hara, Yuuji Kimura and Kaneaki Tsuzaki

Steel Research Center, National Institute for Materials Science, Tsukuba 305-0047, Japan

The annealing behaviour of ultrafine grained steels containing nano-scale dispersed oxides was studied in a temperature range of 600–900°C by means of microstructural observations and hardness measurement. The starting materials with submicrocrystalline structures were developed by mechanical milling of Fe-Fe<sub>3</sub>O<sub>4</sub> powders followed by consolidating bar rolling at 700°C. Depending on the initial oxygen content and the mechanical milling time, the fraction of dispersed oxides varied from 0.3 to 3.0 vol%. During the heating up to 800°C (*i.e.* within the ferrite region), the initial ultrafine grained microstructures were essentially stable against any discontinuous grain growth. The grain coarsening and the softening can be roughly expressed by power-law functions of annealing time. The main mechanism of microstructure evolution that operated during annealing is considered as a normal grain growth accompanied by recovery. The grain coarsening is characterized by a rather high value of the grain-growth exponent of about 20. The grain growth kinetics correlates with the oxide coarsening. The effect of dispersed oxides on the annealing behaviour of submicrocrystalline oxide bearing steels is discussed in some detail.

(Received January 16, 2004; Accepted February 26, 2004)

**Keywords:** ultrafine grained steels, dispersed oxides, mechanical milling, powder consolidation, grain coarsening

## 1. Introduction

Submicrocrystalline materials with an average grain size of below 1 µm are of particular interest to materials scientists and metallurgical engineers. The interest in the ultrafine grained metals and alloys is associated with expected beneficial combination of their mechanical properties, namely high strength with fair plasticity.<sup>1–5)</sup> Such materials are considered as the most promising structural materials for certain engineering applications. However, intensive study of ultrafine grained structures is hampered by the difficulties in materials development. Almost all the methods used to produce materials with submicron grains, like rapid solidification, vapour condensation, severe plastic working, *etc.*,<sup>6–8)</sup> may be utilized for processing of limited sample size or specific alloys, only. In this connection powder metallurgy methods may become the most suitable for production of submicrocrystalline materials. One of such methods is mechanical milling followed by some consolidating working.<sup>9–12)</sup> This processing method allows us to develop sizeable products using almost unlimited variety of materials.

Mechanical ball milling followed by warm consolidating rolling was recently applied for the development of ultrafine grained high-strength steels with nano-scale oxides, which are homogeneously dispersed throughout the ferrite matrix.<sup>13–17)</sup> The final microstructures evolved in the milled iron powders depend strongly on both the period time of mechanical working and the oxygen content. The (sub)grain sizes decrease and (sub)boundary misorientations increase with increasing the milling time<sup>16)</sup> and the amount of oxygen.<sup>15)</sup> Annealing behaviour of worked powders was discussed in terms of recrystallization and/or normal grain growth.<sup>9)</sup> Recrystallization following recovery takes place in the powders milled for relatively short time, resulting in rather coarse grained microstructures. On the other hand, the annealing mechanism of microstructure evolution in the powders milled for sufficiently long period is considered as normal grain growth. In this case, the milled powders maintain their relatively ultrafine grained microstructures

upon further heat treatments. It should be noted that the oxygen content tends to increase with the milling time due to contamination from atmosphere. Therefore, suppression of primary recrystallization in the powders processed by severe plastic working can be caused by a large fraction of strain-induced high-angle (sub)boundaries<sup>18)</sup> as well as due to common pinning effect of dispersed oxide particles.<sup>19)</sup> The grain growth kinetics was shown to correlate with the oxide coarsening in the steel samples with large fraction of dispersed oxides of about 3.0 vol%.<sup>20)</sup> The annealing softening mechanisms were also studied in cold worked oxide-bearing steels with relatively large initial grains.<sup>21)</sup> Primary recrystallization developed partially in samples containing 0.8 vol% of dispersed oxides after rather large pre-strain of above 1.0. In the samples with larger amount of dispersed oxides, static recovery was only the annealing softening process irrespective of cold pre-strain. However, the effect of dispersed oxides on the annealing behaviour of submicrocrystalline steels has not been studied in sufficient details.

The aim of the present work is to study the annealing behaviour of oxide bearing submicrocrystalline steels processed by mechanical milling followed by consolidating rolling. The paper is focussed to clarify the effect of dispersed oxide particles on the grain coarsening mechanisms operating in ultrafine grained bulk material during annealing.

## 2. Experimental Procedure

Three kinds of Fe–O powders with different amount of oxygen, *i.e.* 0.2, 0.6, and 1.5 mass%, were used as the starting materials (Table 1). The average size of powder particles was about 100 µm. The oxygen was in form of Fe<sub>3</sub>O<sub>4</sub> surface

Table 1 Measured Chemical Compositions of Fe–O Powders (mass.%).

Powder	O	N	C	Si	Mn	P	S	Fe
Fe-0.2%O	0.18	0.003	0.002	0.010	0.150	0.010	0.010	bal
Fe-0.6%O	0.58	0.005	0.010	0.009	0.110	0.110	0.007	bal
Fe-1.5%O	1.51	0.008	0.030	0.005	0.003	0.003	0.001	bal

oxide, which comprised about 1 to 8 vol%. The powders were mechanically milled by a planetary ball mill in an argon atmosphere for different times from 20 to 100 hours. After mechanical milling, the worked powders were canned in a steel pipe with an inner diameter of 30 mm and then consolidated by multiple bar rolling at 700°C to a total nominal reduction in area of 86%. Such processing resulted in fully dense bulk rods of about 10 mm in diameter. Table 2 summarises the main structural parameters for consolidated samples that depended on the mechanical milling time and the oxygen content. It should be noted that in the case of relatively short milling time or large initial oxide content, the oxide particles were not dispersed finely and uniformly throughout the ferrite matrix. That is most of the oxygen was in the form of coarse initial oxides. Therefore, only the fine dispersed oxides were analysed; oxide particles larger than 100 nm in size were omitted.

The consolidated bars were cut into 10 mm sample pieces, which were annealed for various times of 1 to 100 hours in an argon muffle furnace at different temperatures from 600 to 900°C, followed by air cooling. Structural analysis was performed on sections parallel to the rolling axis using optical and transmission electron microscopy (TEM) techniques. The average grain size was measured by the linear-intercept method in two directions, *i.e.* along and crosswise to the rolling axis. The distributions and the sizes of the dispersed oxides were studied on typical TEM micrographs combining bright and dark field images, and a total of about 100 particles were analysed in each sample. The foil thickness was calculated by the extinction contour method.<sup>22)</sup> Softening was studied by means of the Vickers hardness test with a load of 4.9 N.

### 3. Results

Microstructures (namely the average grain sizes) evolved in the present oxide bearing steels after consolidation demonstrate a complex dependence on the mechanical milling time and the oxygen content (Table 2). It was discussed that the volume fraction of dispersed oxides ( $F_{D.O.}$ ) has a dominant role in the final microstructure formation after consolidating working.<sup>16,17)</sup> In the present paper, therefore, the annealing behaviour of various Fe–O steel samples is considered with reference to the volume fraction of nano-scale dispersed oxides.

#### 3.1 Isochronal annealing

Figure 1 shows typical annealed microstructures evolved in the sample with 3.0 vol% of dispersed oxides after

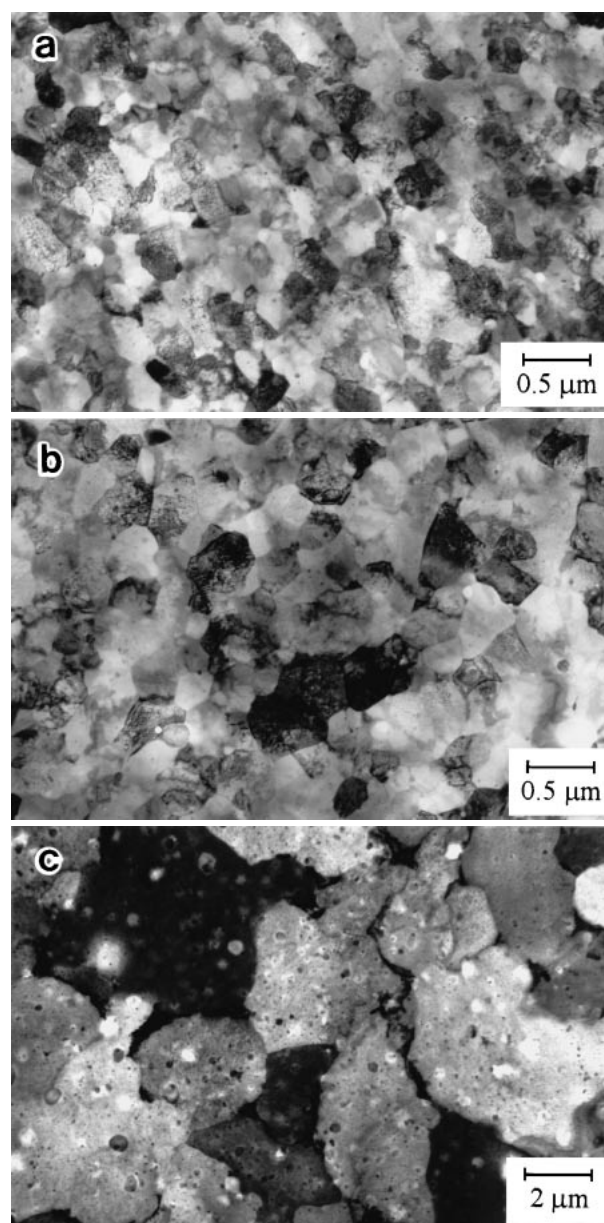


Fig. 1 Typical microstructures developed in Fe–O steel with 3.0 vol% of dispersed oxides; (a) as processed state; (b) annealed at 800°C for 1 hour; (c) annealed at 900°C for 1 hour.

isochronal annealing for 1 hour at temperatures of 800 and 900°C, including the initial as-processed microstructure with ultrafine grains, Fig. 1a, that developed after consolidation of worked powder. The structural changes during annealing depend on the heating temperature. Annealing at temperatures below 800°C does not cause any significant changes in the initial ultrafine grained microstructure, while heating to 900°C (just above  $A_3$  temperature) results in substantial grain coarsening. Such a drastic effect of annealing temperature was considered to result from the phase transformation.<sup>23,24)</sup> It was shown that fine oxide particles are effective to retard grain growth in the austenite range as well as in the ferrite range.<sup>23)</sup> The average grain size in Fig. 1c is about 2.0 μm, which can be also considered as an ultrafine grained microstructure. However, referring to the as-processed and annealed microstructures in Figs. 1a and b, where the grains

Table 2 Some microstructural parameters after consolidation of mechanically milled Fe–O steels.

Oxygen content, %	0.2	0.6	0.6	1.5
Milling time ( <i>t</i> ), hours	100	20	100	100
Average grain size ( <i>D</i> ), μm	0.7	1.2	0.35	0.2
Size of dispersed oxides ( <i>d</i> ), nm	9	13	10	11
Volume fraction of dispersed oxides ( $F_{D.O.}$ ), %	0.8	0.3	2.0	3.0



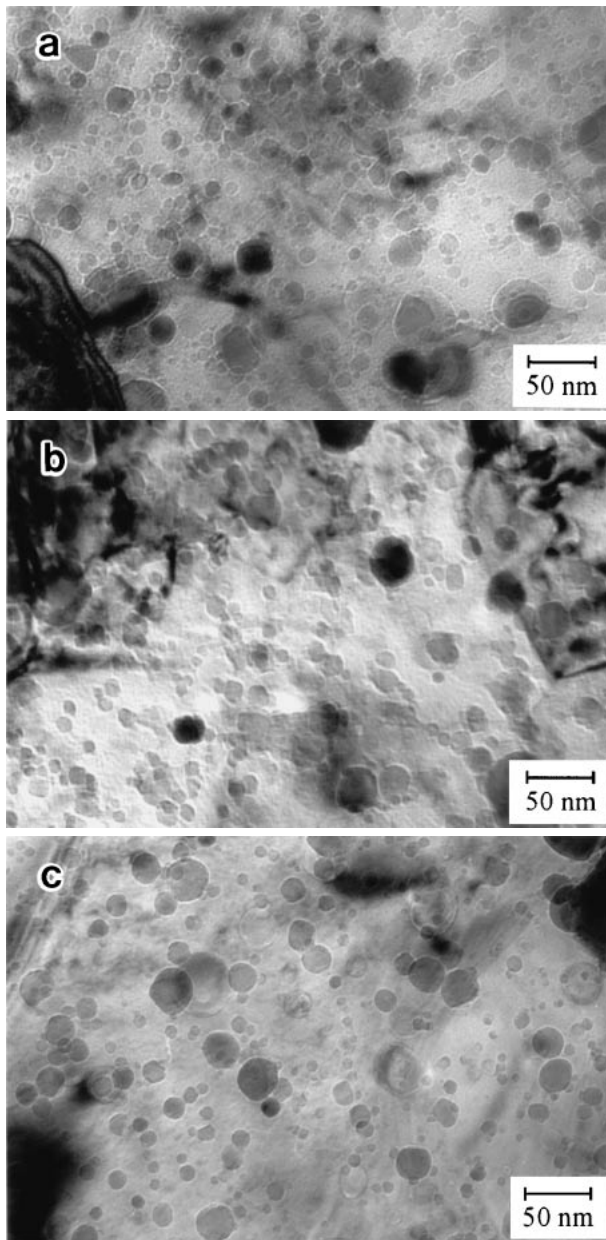


Fig. 2 Dispersed oxides in the Fe–O steel samples with 3.0 vol% of dispersed oxides; (a) as-processed state, (b) and (c) annealed for 1 hour at 800 and 900°C, respectively.

are about 10 times finer, it is clearly seen that the ferrite-austenite-ferrite transformation may completely break the initial submicrocrystalline ferrite structures.

On the other hand, the distribution of dispersed oxides does not change remarkably during 1 hour annealing irrespective of annealing temperature, as it can be seen in Fig. 2. The size of dispersed oxides after annealing is almost the same as that evolved in the as-processed sample even after heating to such a high temperature as 900°C (*cf.* Figs. 2a and c).

Strictly speaking, it is not surprising that matrix-type microstructures with rather large fraction of nano-sized dispersed particles, which are homogeneously distributed throughout, are quite stable against rapid grain coarsening during the heating.<sup>25,26</sup> In general, the microstructural homogeneity of consolidated powders should depend on the

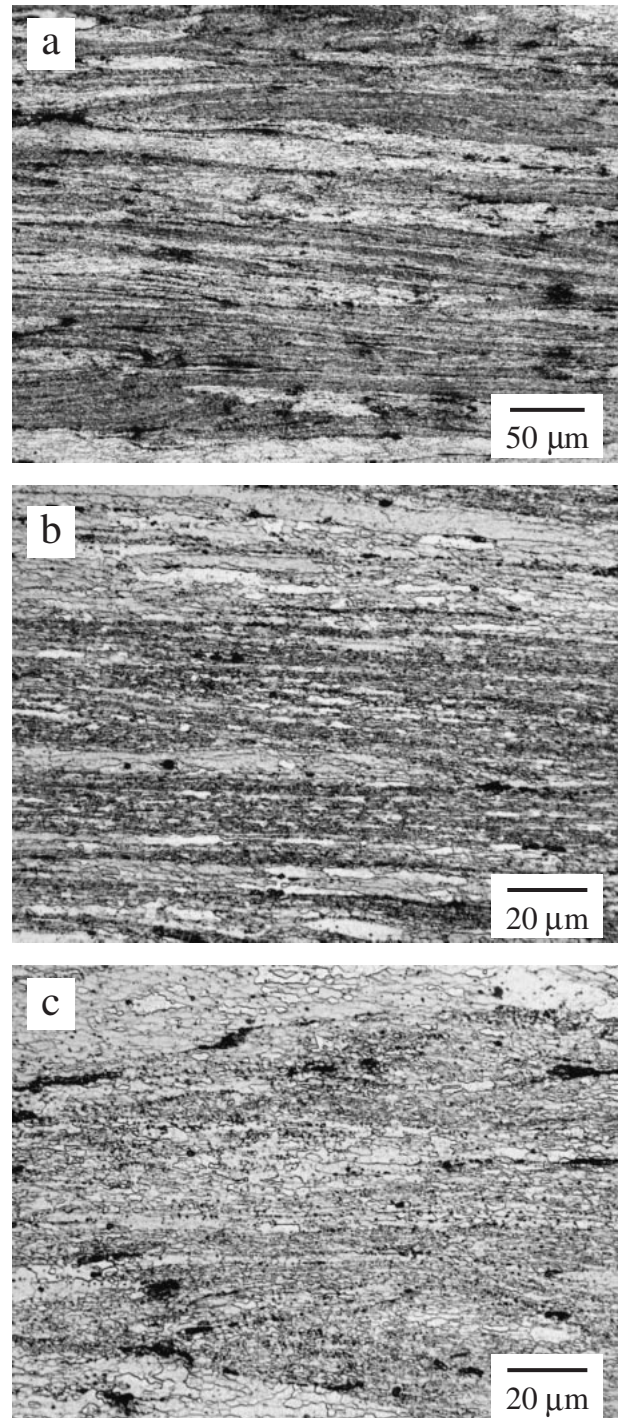


Fig. 3 Effect of annealing on the ultrafine grained microstructures in Fe–O steel with 0.3 vol% of dispersed oxides; (a) as-processed microstructure; (b) annealed at 600°C for 1 hour; (c) annealed at 800°C for 1 hour.

intensity of powder processing. Some variations in distribution of dispersed oxides was discussed to result in the evolution of coarse pan-caked recrystallized grains in the cold worked Fe–O steels with 0.8 vol% of dispersed oxides.<sup>21</sup> Figure 3 shows typical optical micrographs for the samples with 0.3 vol% of dispersed oxides (the shortest milling time, *s.* Table 2) in the as-processed state and annealed for 1 hour at 600 and 800°C. In spite of certain macro-scale heterogeneity associated with some un-milled coarse initial oxides, the annealed microstructures are

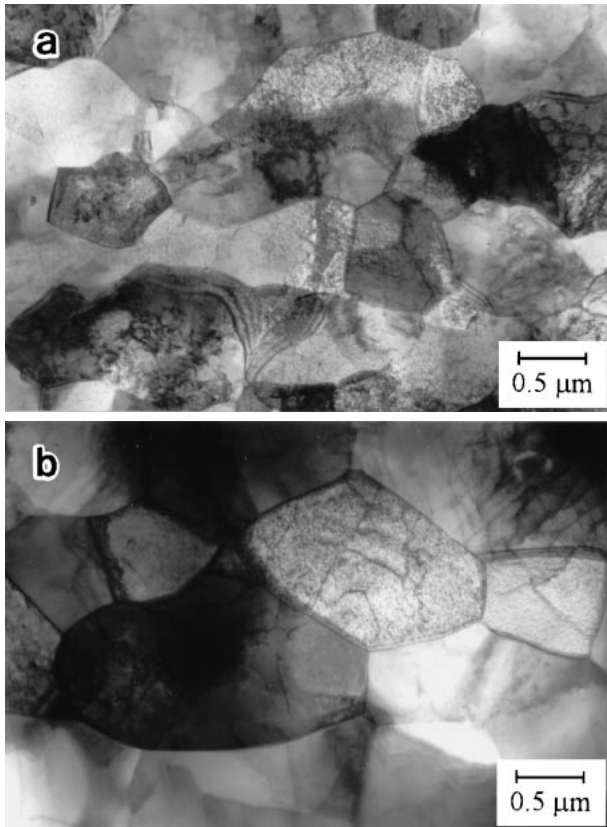


Fig. 4 Typical annealed microstructures evolved in Fe–O steels with 0.3 vol% of dispersed oxides; (a) annealing at 600°C for 1 hour; (b) annealing at 800°C for 1 hour.

composed of almost uniform fine grains. TEM micrographs corresponding to those in Figs. 3b and c are shown in Fig. 4. The annealed grain sizes of 1–2 μm are quite close to that of 1.2 μm in the initial as-processed state before annealing.

Figure 5 shows the effect of the annealing temperature on the specimen hardness (Hv) and the average grain size ( $D$ ) for various Fe–O samples with different fractions of dispersed oxides. At temperatures of 600–800°C, grain coarsening hardly takes place, and the hardness is just below its value in the as-processed state. Such behaviour is clearly observed for all studied Fe–O samples irrespective of the volume fraction of dispersed oxides. Increase of the dispersed oxide fraction resulted in decrease of the initial grain size; however, the further annealing behaviour seems to be invariant of the fraction of dispersed oxides. It is concluded that the ultrafine grained microstructures developed in the consolidated Fe–O steels with volume fraction of dispersed oxides of above 0.3% are quite stable against any discontinuous recrystallization, and only slow grain growth accompanied by recovery takes place during annealing in the ferrite range.

### 3.2 Grain growth behaviour

Figure 6 shows typical microstructures developed in the samples with different volume fractions of dispersed oxides during annealing at 700°C. In spite of rather large difference in the initial grain sizes in the samples with 0.3 and 3.0 vol% of dispersed oxides, the long-time annealing for 100 hours does not lead to any remarkable differences in grain growth

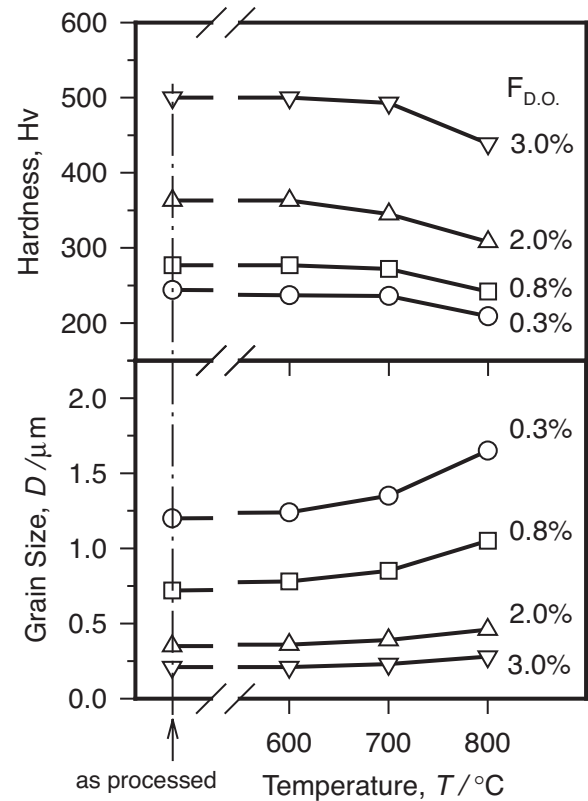


Fig. 5 Effect of annealing temperature on the hardness and the grain size of Fe–O steels with different fractions of dispersed oxides ( $F_{D.O.}$ ).

kinetics. The samples annealed for 1 and 100 hours can be characterised by almost the same microstructures (Fig. 6). The long-time annealing for 100 hours results in slight increase in the average size of dispersed oxides to about 13 nm in the samples with  $F_{D.O.}$  of 3.0 vol%, and to about 17 nm in the samples with  $F_{D.O.}$  of 2.0 and 0.8 vol%. It should also be noted that the long-time annealing, which leads to a certain grain coarsening, does not remove the dislocation substructures like interior dislocations. The latter ones are clearly visible in TEM images, *e.g.* Fig. 6b.

The variations in the room-temperature hardness and the average grain size upon annealing at 700°C are shown in Fig. 7 in double-logarithmic scale for the samples with different fractions of dispersed oxides. Both the hardness and the grain size can be expressed by power-law functions of the annealing time. For all the samples, the annealing time dependence of the hardness can be represented by a power-law function with roughly the same time exponent of about  $-0.04$  irrespective of the fractions of dispersed oxides. Similar to the hardness change, the average grain size increases continuously with the annealing time, and the grain growth kinetics does not depend on the fraction of dispersed oxides. This suggests that the annealing behaviour of the ultrafine grained steels with the grain sizes of about 0.2–2.0 μm containing of 0.3–3.0 vol% of dispersed oxides can be characterised by the operation of the same structural mechanism controlling the grain coarsening upon heating.

The annealed grain size is generally related to the annealing time ( $t$ ) as:<sup>27)</sup>  $D = At^{1/n}$ , where  $A$  and  $n$  are constants. According to original theoretical analysis of the



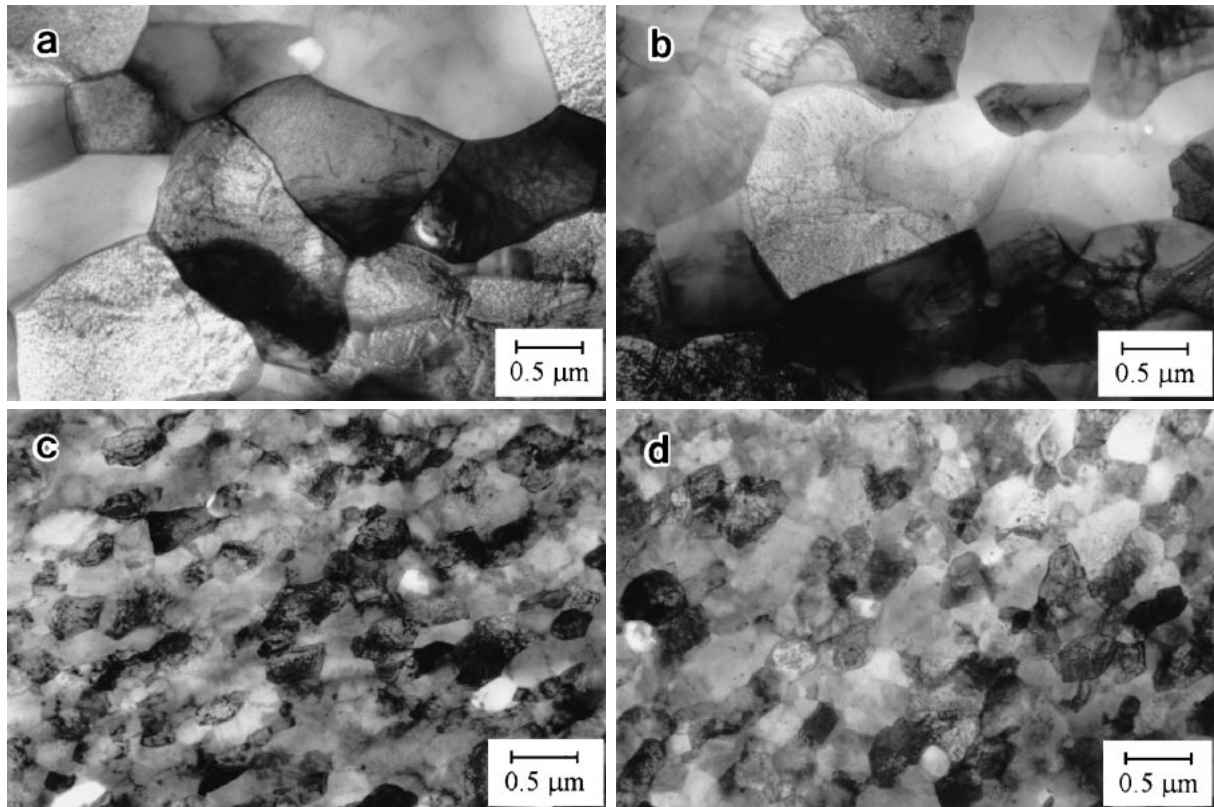


Fig. 6 Typical microstructures developed in Fe–O steels with different fractions of dispersed oxides ( $F_{D.O.}$ ) during annealing at 700°C; (a)  $F_{D.O.} = 0.3\%$ , 1 hour annealing; (b)  $F_{D.O.} = 0.3\%$ , 100 hour annealing; (c)  $F_{D.O.} = 3.0\%$ , 1 hour annealing; (d)  $F_{D.O.} = 3.0\%$ , 100 hour annealing.

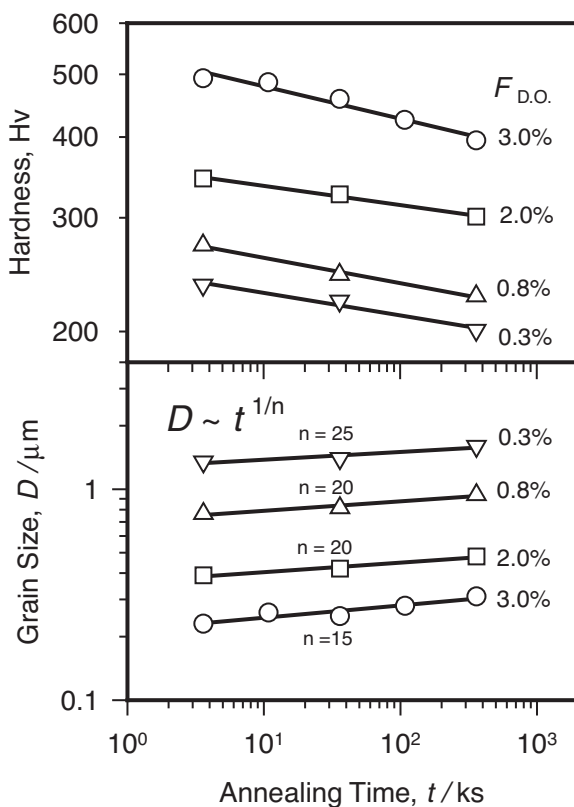


Fig. 7 Variations in the room-temperature hardness (Hv) and the grain size ( $D$ ) with annealing at 700°C for ultrafine grained Fe–O steels with different fractions of dispersed oxides ( $F_{D.O.}$ ).

grain growth in pure single-phase materials,<sup>26)</sup> the grain growth exponent ( $n$ ) is equal to 2. When the grain growth is limited by the pinning effect from dispersed particles,  $n = 3$  for particle coarsening controlled by volume diffusion,<sup>28)</sup> and  $n = 4$  for particle coarsening controlled by diffusion along (sub)grain boundaries.<sup>29)</sup> In the present study, the rather large value of the grain growth exponent of  $20 \pm 5$  is obtained for all the samples with different fractions of dispersed oxides. The measured grain growth exponent usually ranges from 2 to 10.<sup>26,30,31)</sup> The relatively large values of the grain growth exponent of around 10 were reported for ferrite containing cementite particles<sup>31)</sup> and low-carbon steel processed by severe plastic working<sup>32)</sup> (in the latter study, annealing was carried out at relatively low temperature of 480°C).

#### 4. Discussion

The present results suggest that the annealing behaviour of the submicrocrystalline steels with different fractions of dispersed oxide particles varied from 0.3 to 3.0 vol% is characterised by continuous grain growth with quite slow coarsening kinetics. The grain size in multiphase matrix-type metallic materials depends on the size and volume fraction of second-phase particles due to the so-called pinning effect.<sup>19,26)</sup> The maximum retarding force leads to a cessation of grain growth when  $D = Kd/F_{D.O.}$ , where  $K$  is a factor depending on various structural parameters, and  $d$  is the particle size. Figure 8 presents the relationship between the grain size and the dispersed oxides for the as-processed

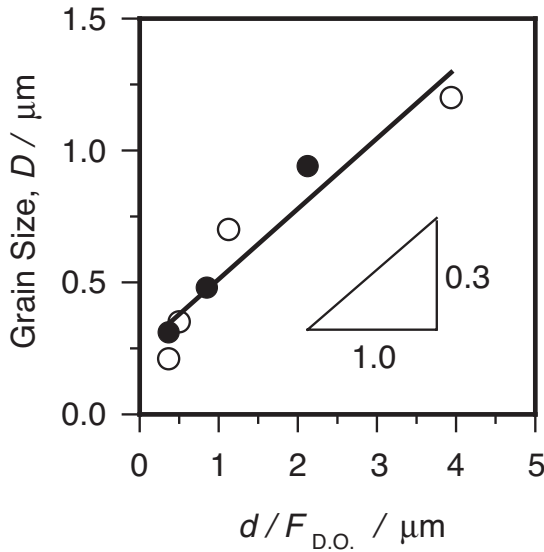


Fig. 8 Effect of dispersed oxides on the grain size in Fe–O steels. Open and closed symbols correspond to as-processed and annealed samples, respectively.

samples and the samples annealed at 700°C for 100 hours. The  $D$  vs  $d/F_{D.O.}$  dependence can be roughly represented by a linear function with the slope of about 0.3. This is consistent with numerous studies<sup>25,33–35</sup> that predict the  $K$  values from 0.16 to 0.67. It is concluded, therefore, that the grain growth in the studied Fe–O steels during annealing correlates with the coarsening of the dispersed oxides particles.

Let us consider the probable mechanism controlling the microstructure evolution in the present Fe–O steels during annealing. The mobility of grain boundaries ( $M$ ) depends on the temperature ( $T$ ) and can be commonly expressed as:<sup>26</sup>  $M = M_0 \exp(-Q/(RT))$ , where  $M_0$  is a constant,  $Q$  is the apparent activation energy for the process, and  $R$  is the universal gas constant. In the present case, the annealed grain sizes do not differ very much from the original ones ( $D_0$ ) corresponding to the as-processed state. Therefore, the mobility of grain boundaries during annealing can be roughly related to the change of grain sizes,  $\Delta D = D - D_0$ . The relationship between the  $\Delta D$  and  $1/T$  is represented in Fig. 9 in semi-logarithmic coordinates. From this figure, almost the same values for apparent activation energy of about 85 ~ 110 kJ/mol can be derived for all the Fe–O samples. The oxygen diffusion in iron seems to be the main factor controlling oxide coarsening, and therefore the grain growth, in the studied material. The activation energy for oxygen diffusion in iron was reported from 92 kJ/mol<sup>36</sup> to 167 kJ/mol.<sup>37</sup> Such variation in the activation energies may be associated with the difference in the dominant diffusion mechanisms. The diffusion along (sub)grain boundaries (or pipe diffusion) is characterised by lower values of the activation energy than the volume diffusion

Generally, the strengthening from dispersed particles ( $\tau_0$ ) is inversely proportional to the inter-particle distance ( $l$ ), for instance:<sup>38</sup>  $\tau_0 = (Cgb/2\pi(l-d)) \ln(d/5b)$ , where  $C$  is a constant,  $G$  is the shear modulus, and  $b$  is the Burgers vector. For randomly distributed oxide particles, the inter-particle

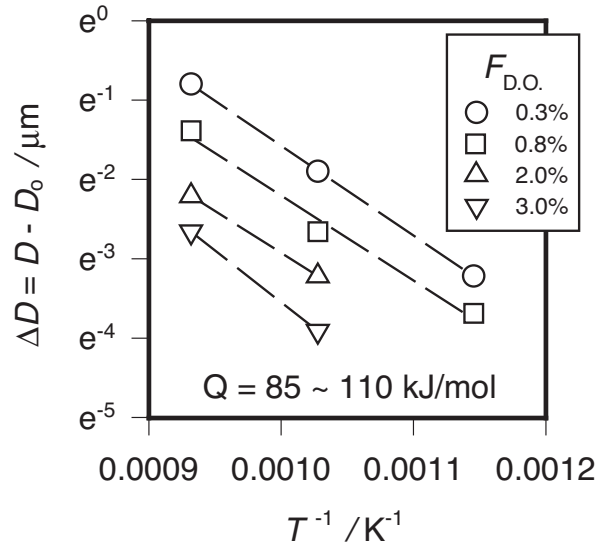


Fig. 9 Grain growth during annealing of Fe–O steels with various fractions of dispersed oxides ( $F_{D.O.}$ ).

distance can be related to the oxide particle size and their fraction as:<sup>26</sup>  $l = d(24F_{D.O.}/\pi)^{-0.5}$ . It was mentioned above that the average annealed grain size in the studied Fe–O steels varies directly as the size of dispersed oxides, therefore,  $F_{D.O.} \sim d/D$  (s. Fig. 8). This results in the following qualitative expression for dispersion strengthening:  $\tau_0 \sim (Dd)^{-0.5}$ . If the particle sizes do not change significantly, the dispersion strengthening should be almost similar to the strengthening by grain refinement, *i.e.* the Hall-Petch relationship.<sup>39</sup> Figure 10 shows the relationship between the hardness and the grain size for the ultrafine grained steels; the present data are combined with previously published results.<sup>13,24</sup> This figure also represents the data extrapolated from grain size dependence of yield stress ( $\sigma_y$ ) for conventional coarse grained iron,<sup>40</sup> on the assumption that  $Hv \approx 2.6 \sigma_y$ . It is clearly seen that the hardness can be expressed by a linear function of the inverse square root of the grain size for

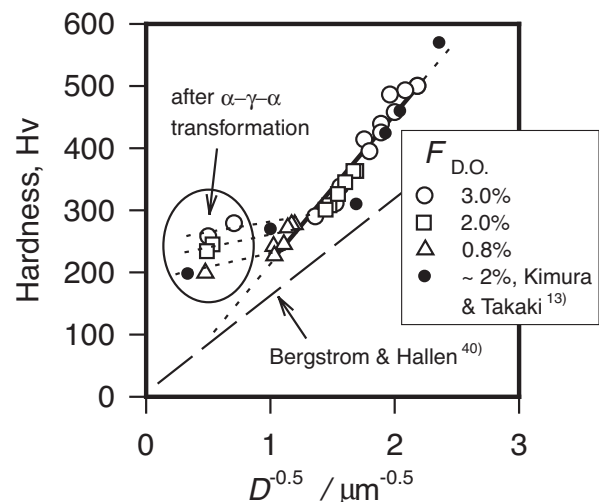


Fig. 10 Relationship between the average grain size and the hardness for the ultrafine grained Fe–O steels.

the samples annealed in the ferrite region, including the as-processed state. An increased slope of the  $H_v$  vs  $D^{-0.5}$  plot for these samples as compared to that for the coarse grained iron can result from an additional strengthening effect of the dispersed oxides. Using  $G = 64$  GPa,  $b = 0.25$  nm and  $d$  from Table 2, the  $\tau_0$  for the samples with the volume fractions of dispersed oxides of 0.8% and 3.0% can be evaluated as about 200 MPa and 450 MPa, respectively. On the other hand, the samples annealed at higher temperatures, namely those affected by the  $\alpha - \gamma - \alpha$  phase transformation demonstrate higher strength than it could be expected. This is associated with the change of structural mechanisms responsible for microstructure evolution. The phase transformation provides specifically high driving force for the grain boundary migration; while the size of dispersed oxides do not change remarkably (s. Fig. 2), that can be simply explained by a lowered diffusivity in the close-packed *fcc* lattice, especially upon a relatively short-time annealing.

## 5. Conclusions

The effect of nano-sized oxides on the annealing behaviour of submicrocrystalline Fe–O steels was studied at temperatures of 600 ~ 900°C. The main results can be summarised as follows.

(1) Homogeneously dispersed oxides with their volume fractions ranging from 0.3 to 3.0% are very effective for stabilization of ultrafine grained ferrite matrices. The ultrafine grained Fe–O steels are essentially stable against any rapid discontinuous grain growth during annealing at temperatures up to 800°C, *i.e.* within the ferrite region.

(2) The annealing behaviour at  $T \leq 800^\circ\text{C}$  is mainly associated with the operation of continuous grain growth, which correlates with the coarsening of dispersed oxides. The grain growth can be characterised by a relatively large grain growth exponent of about 20 and apparent activation energy of about 100 kJ/mol.

(3) The strengthening of as-processed and annealed ultrafine grained Fe–O steels with different fractions of dispersed oxides varying in the range of 0.3 ~ 3.0 vol% obeys the Hall-Petch-like relationship, when the final microstructures are resulted from the continuous grain growth.

## REFERENCES

- 1) R. Z. Valiev, R. K. Islamgaliev and I. V. Alexandrov: *Progr. Mater. Sci.* **45** (2000) 103–189.
- 2) D. G. Morris: *Science of Metastable and Nanocrystalline Alloys Structure, Properties and Modelling*, ed. by A. R. Dinesen *et al.*, (Riso National Laboratory, Roskilde 2001) pp. 89–104.
- 3) R. Valiev: *Nature* **419** (2002) 887–888.
- 4) Y. Wang, M. Chen, F. Zhou and E. Ma: *Nature* **419** (2002) 912–915.
- 5) C. C. Koch: *Scr. Mater.* **49** (2003) 657–662.
- 6) H. Gleiter: *Progr. Mater. Sci.* **33** (1989) 223–315.
- 7) C. Suryanarayana: *Int. Mater. Rev.* **40** (1995) 41–64.
- 8) R. Z. Valiev, I. V. Alexandrov, Y. T. Zhu and T. C. Lowe: *J. Mater. Res.* **17** (2002) 5–8.
- 9) Y. Kimura and S. Takaki: *Mater. Trans., JIM* **36** (1995) 289–296.
- 10) C. C. Koch: *NanoStructured Mater.* **9** (1997) 13–22.
- 11) Y. Kimura, H. Hidaka and S. Takaki: *Mater. Trans., JIM* **40** (1999) 1149–1157.
- 12) C. Suryanarayana: *Progr. Mater. Sci.* **46** (2001) 1–184.
- 13) Y. Kimura and S. Takaki: *Proc. 7th Int. Conf. on Composites Engineering*, ed. by D. Hui, (International Community for Composites Engineering, University of New Orleans, 2000) pp. 461–462.
- 14) Y. Sakai, M. Ohtaguchi, Y. Kimura and K. Tsuzaki: *Ultrafine Grained Materials*, ed. by R. S. Mishra *et al.*, (TMS, Warrendale, 2000) pp. 361–370.
- 15) A. Belyakov, Y. Sakai, T. Hara, Y. Kimura and K. Tsuzaki: *Metall. Mater. Trans. A* **32A** (2001) 1769–1776.
- 16) A. Belyakov, Y. Sakai, T. Hara, Y. Kimura and K. Tsuzaki: *Metall. Mater. Trans. A* **33A** (2002) 3241–3248.
- 17) K. Tsuzaki: *Mater. Sci. Forum* **426–432** (2003) 2771–2776.
- 18) F. J. Humphreys: *Acta Mater.* **45** (1997) 4231–4240.
- 19) C. S. Smith: *Trans. ASM* **175** (1948) 15–51.
- 20) A. Belyakov, Y. Sakai, T. Hara, Y. Kimura and K. Tsuzaki: *Metall. Mater. Trans. A* **34A** (2003) 131–138.
- 21) A. Belyakov, Y. Sakai, T. Hara, Y. Kimura and K. Tsuzaki: *Scr. Mater.* **48** (2003) 1463–1468.
- 22) D. B. Williams and C. B. Carter: *Transmission Electron Microscopy*, (Plenum Press, New York, 1996) pp. 369–371.
- 23) M. Ohtaguchi, K. Tsuzaki and K. Nagai: *Recrystallization and Related Phenomena*, ed. by T. Sakai and H. G. Suzuki (The Japan Institute of Metals, Sendai, 1999) pp. 495–500.
- 24) A. Belyakov, Y. Sakai, T. Hara, Y. Kimura and K. Tsuzaki: *Recrystallization and Grain Growth*, ed. by G. Gottstein and D. A. Molodov, (Springer-Verlag, Berlin, 2001) pp. 537–542.
- 25) E. Hornbogen and U. Koster: *Recrystallization of Metallic Materials*, ed. by F. Haessner, (Verlag, Stuttgart, 1978) pp. 159–194.
- 26) F. J. Humphreys and M. Hatherly: *Recrystallization and Related Annealing Phenomena*, (Pergamon Press, Oxford, 1996) pp. 235–325.
- 27) P. A. Beck: *J. Appl. Phys.* **18** (1947) 1028–1029.
- 28) M. Hillert: *Acta Metall.* **13** (1965) 227–238.
- 29) A. J. Ardell: *Acta Metall.* **20** (1972) 601–609.
- 30) G. Wiener: *Trans. ASM* **44** (1952) 1169–1185.
- 31) P. Hellman and M. Hillert: *Scandinavian J. Metall.* **4** (1975) 211–219.
- 32) K. T. Park, Y. S. Kim and J. G. Lee and D. H. Shin: *Mater. Sci. Eng. A* **A293** (2000) 165–172.
- 33) T. Gladman: *Proc. Roy. Soc. London* **294A** (1966) 298–309.
- 34) A. K. Koul and F. B. Pickering: *Acta Metall.* **30** (1982) 1303–1308.
- 35) P. A. Manohar, M. Ferry and T. Chandra: *ISIJ Int.*, **38** (1998) 913–924.
- 36) J. Takada, S. Yamamoto and M. Adachi: *Z. Metallkd.* **77** (1986) 6–11.
- 37) R. Barlow and P. J. Grundy: *J. Mater. Sci.* **4** (1969) 797–801.
- 38) S. Onaka: private communication.
- 39) E. O. Hall: *Proc. Phys. Soc.* **B64** (1951) 747–753.
- 40) Y. Bergstrom and H. Hallen: *Met. Sci.* **17** (1983) 341–347.